Geochemistry of the Lake Chad Tributaries Under Strongly Varying Hydro-climatic Conditions

A. Mahamat Nour, Christine Vallet-Coulomb, Camille Bouchez, P. Ginot, J. Doumnang, F. Sylvestre, P. Deschamps

Geochemistry of the Lake Chad Tributaries Under Strongly Varying Hydro-climatic Conditions

A. Mahamat Nour, C Vallet-Coulomb, Camille Bouchez, P. Ginot, J. Doumnang, F. Sylvestre, P. Deschamps

Geochemistry of the Lake Chad tributaries under strongly varying hydro-climatic conditions

Mahamat Nour A.[1,2], Vallet-Coulomb C.[1], Bouchez C.[1,4], Ginot P.[3], Doumnang J.C.[2], Sylvestre F.[1], Deschamps P.[1]

[1]Aix Marseille Université, CNRS, IRD, Collège de France, INRA, CEREGE, Aix-en-Provence, France
[2]Université de N'Djaména –Laboratoire HydroGéoscience et Réservoir, N'Djaména, Tchad
[3]Université Grenoble Alpes, IRD, CNRS. Institut des Géosciences de l'Environnement, UMR5001, Grenoble, France
[4] Univ Rennes, CNRS, Géosciences Rennes, UMR 6118, 35000 Rennes, France.

Email: mahamatnour@univ-ndj.td

Abstract

The Lake Chad Basin (LCB) is one of the main endorheic basins in the world and has undergone large level and surface variations during the last decades, particularly during the Sahelian dry period in the 1970s and the 1980s. The Chari-Logone River system covers 25% of the LCB but accounts for up to 82% of the Lake Chad water supply. The aim of this study is to investigate the dissolved phase transported by the Chari-Logone system, in order (i) to elucidate the origin and the behavior of major elements and the weathering processes in the watershed; (ii) to estimate the total dissolved flux, its variability over the last decades and the driving factors. To do so, samples were collected monthly between January 2013 and November 2016 at three representative sites of the basin: in the Chari River in "Chagoua", in the Logone River in "Ngueli" just before the confluence of both rivers, and at a downstream site in "Douguia", 30 km after the confluence. Concentrations in major elements displayed significant seasonal variations in the Chari and Logone waters. At the seasonal time scale, the comparison between the concentrations of chemical elements and the flow rates showed a hysteresis loop. This hysteresis behavior correspond to a variable contribution over time of two water bodies, fast surface water, and slow groundwater, the latter carrying higher concentrations and Ca/Na ratio, which may result from the contribution of pedogenic carbonate weathering to the dominant signature of silicate weathering. On the other hand, similar average concentrations are observed in the Chari and Logone rivers, despite contrasted annual runoff. In addition, an interannual stability of ionic concentrations was observed in the Chari-Logone river during the flood regime, both during the years covered by our monitoring (2013-2016) and during the pre-drought period (1969, 1972 et 1973). This situation corresponds to a chemostatic behavior, where the annual river discharge is the main factor controlling the interannual variation of chemical fluxes.

Keywords: Lake Chad basin, chemical fluxes, silicate weathering, strontium

Introduction

Located at the southern edge of the Sahara, in the central Sahel, Lake Chad is a large freshwater body that provides resources for 49 million people living around. This lake has a long history of alternating wet and dry periods spanning from millennia to the annual and seasonal time scales (Schuster et al. 2005; Sylvestre 2014). The high variability of the lake level, and associated lake extension, reflects its high sensitivity to climatic conditions, mainly due to its endorheic context. Located in the southern part of the Lake Chad Basin (LCB), the Chari - Logone River system is today the only active hydrological catchment. It represents 25% of the total LCB surface, but accounts for up to 82% of the Lake Chad water supply (Bouchez et al. 2016). Therefore, as Lake Chad is the outlet of elemental fluxes carried by the Chari-Logone River, understanding its hydro-geochemical behavior and what control these fluxes is crucial to better characterize the chemical evolution of the lake.

River geochemistry reflects the various weathering processes that affect the Earth's surface (e.g. Probst et al. 1992; Louvat and Allègre 1997; Viers et al. 2000; Meybeck 2003; Ollivier et al. 2010; Chorover et al. 2017; Koger et al. 2018). Among the numerous studies that aimed at quantify weathering rates and understanding the parameters that control their variations, special attention was paid to silicate weathering, which, while pumping atmospheric CO_2, plays a particular role in the global carbon cycle (e.g. Gaillardet et al. 1999; Amiotte Suchet et al. 2003; Hartmann et al. 2009; Mortatti & Probst 2003).

Tropical environments occupy nearly a third of the total area of the continents; but they are under-represented in regional geochemical studies. Especially in Tropical Africa, only a few studies have focused on such geochemical processes i.e. weathering. The only African basins that have been investigated are those of Congo (Probst et al. 1992; Négrel et al. 1993), Nyong (Viers et al. 2000), Niger (Picouet et al. 2002), South Africa (Meybeck et al. 1996) and Sassandra (Agri et al. 2010). These studies have estimated weathering fluxes generally below the world average rate. However, tropical environments are expected to encounter large hydrological perturbations in the coming decades with unknown consequences on weathering fluxes.

From Sahel band, very few studies have been carried out and especially on the Chari-Logone River system, which is one of the main water networks. Roche (1980) provided the first observations describing the water physico-chemistry of Chari and Logone. Carmouze (1976) and Gac (1980) also studied the transport of salt, in order to describe the lake's chemical

equilibrium and to identify the mechanisms that regulate it. But since these early works, no significant study has attempted to characterize the dissolved load of the Chari-Logone system. The aim of the present study was to characterize the weathering processes that control the chemical load and fluxes towards Lake Chad, and to analyze their link with climate variations. Monthly sampling was conducted in each of the main sub-basins of the lake, the Logone and the Chari sub-basins. The dominant contribution of silicate weathering was assessed, and the contribution of each sub-basin was estimated. The estimated total weathering flux was compared to data obtained in the early 1970s and to other neighboring African watersheds.

1. Study area

1.1. Geological and geomorphological context

The Chari-Logone catchment (613 10^3 km²) is bordered by moderate elevation mountain ranges (285 - 1400m): Adamaoua (South-West), Kaggas (South), Ouaddai (East) and Guera (North), and remains mainly flat elsewhere, with areas seasonally flooded along the river courses (Fig. 1). The main geological features of the Chari and Logone basins show two main units (Louis 1970; Gac 1980). In the South and North-East, the Precambrian basement outcrops, mainly represented by granites (46%), and different metamorphic rocks (e.g. migmatites, quartzites, gneiss, schists and micaschists). Ferralitic sesquioxide soils are derived from these formations (Pias 1968). The Center and North-Western parts are covered with sedimentary series of the Tertiary (Continental Terminal sandstone formation) and late Quaternary (fluviatile or fluvial-lacustrine formations). While the sedimentary formations constitute the main aquifer systems (Schneider & Wolf 1992), groundwater also circulates in hard rocks of the Precambrian basement (Schneider & Wolf 1992) supporting baseflow in the upper part of the Chari-Logone catchment (Bouchez et al. 2019).

1.2. Climate and hydrography

Dominated by the seasonal variation of the intertropical convergence zone (ITCZ), the climate of the Chari-Logone catchment area reflects the confluence between two air masses: the south-western humid monsoon of oceanic origin and the north-easterly dry Harmattan of continental origin. Thus, depending on the season, from south to north, the Chari-Logone basin shows a gradual transition from humid to semi-arid conditions. The average precipitation rate, calculated from the General Directorate of National Meteorology of Chad (DGMN) dataset, is

544 mm at N'Djamena, between 1984 and 2014. The rainy season starts in May and ends in October and most precipitation falls in July and August (Fig. 2a). The evaporation rates show a well-marked seasonal cycle following the air temperature cycle (Fig.2b).

The basin is drained by two main hydrographic networks, the Logone and the Chari rivers. The Logone river, with a length of 1000 km, originates in the Adamawa plateau in Cameroon, with an altitude ranging from 305 to 835 m (Cabot 1965; Gac 1980). The Chari Basin covers an area of approximately 523 10^3 km^2. The convergence of the Chari and the Logone rivers is located in N'Djamena, 110 km upstream of Lake Chad, (Fig. 1). The total area of the Logone catchment is 90 10^3 km^2 at the confluence with the Chari. The Chari starts in the Central African Republic at an altitude between 500 and 600 m. It flows nearly 1200 km from the Central African Republic to the Lake Chad. The Chari-Logone receives water input from groundwaters of the Precambrian basement upper basin while in the lower part the Chari-Logone water flows from the river towards the Quaternary Aquifer (Bouchez et al. 2019). The Chari-Logone baseflow discharge is supported by only 12% of the catchment (Bouchez et al. 2019).

2. Data acquisition

2.1. Sampling

River waters were sampled every month during two periods, between January 2013 and August 2014, and between July 2015 and November 2016. They were collected at three sites (Fig. 1): (i) the Chari at Chagoua (N'Djamena, 12°05'16''N and 15°04'52''E), (ii) the Logone at Nguéli (N'Djamena, 12°04'08''N and 15°03'14''E), both sites located upstream of the confluence, and (iii) the Chari-Logone at Douguia (12°38'24''N and 14°49'37''E), located 30 km downstream of the confluence.

The physico-chemical parameters (T, pH and electrical conductivity) were measured in situ (Table 1-3). The waters were first filtered on a 0.45µm nylon membrane and cellulose membrane and stored in pre-cleaned HDPE bottles kept in the dark and in a cold room. Water samples for cation analysis were then acidified with ultra-pure nitric acid. Alkalinity was measured few hours after sampling for all samples by colorimetric titration, and three replicates were performed for each sample, which allowed a reproducibility better than 5%. In table 1-3 we have the values.

2.2. Geochemical analysis

Major dissolved elements and Sr concentration were analyzed at the Institute of Environmental Geosciences (IGE) in Grenoble by ion chromatography, calibrated to measure low concentrations as well as at the European Center for Research and Education in Environmental Geosciences (CEREGE). Strontium isotopes were analyzed with a Neptune + plasma-source multi-collector mass spectrometer (MC ICP-MS) on sixty river samples. A preliminary separation and purification of the strontium was carried out. For each sample, a volume of water corresponding to about 200 ng of Sr was evaporated. The strontium preparation and separation steps were carried out using the Sr-Spec specific resin on a 200 µl column. The fraction was evaporated and then attack with HNO_3 + H_2O_2 to mineralize any organic residues of the Sr-Spec resin. Then, for the MC-ICP-MS analysis, dry samples were taken up and dissolved with HNO_3 1%. The internal measurement accuracy of the $^{87}Sr/^{86}Sr$ ratio is ± 8 x 10^{-6} (2σ). The reproducibility of the $^{87}Sr/^{86}Sr$ ratio measurements was tested by repetitive analysis of the international standard NBS 987 ($^{87}Sr/^{86}Sr$ ratio: 0.710240 ± 0.00002, 2σ, n = 59). This value is similar to the accepted value of 0.710248 ± 0.000011 (Thirlwall 1991). Repeated preparations and measurements of a water sample from Lake Chad labelled TCH2 were also carried out to check long term consistency of the overall Sr isotope procedure.

2.3. Hydrological data

Daily river flows were measured by the Water Resource Directorate (DRE) between 2013 and 2016 at the same locations as the sampling sites: N'Djamena TP on the Chari-Logone, Chagoua on the Chari and Ngueli on the Logone. No data were available for the Logone at Ngueli between 2013 and 2014. The Chari -Logone regime is characterized by a flood period that starts with the rainy season in August and lasts until October when it reaches its maximum (Fig. 2b). The recession starts at the end of October and lasts until December, and low discharges continue from January to June. There is a time lag of two months between the maximum of rainfall and the maximum of discharge measured for the Chari-Logone at N'Djamena (Fig. 2b). The average annual flows in 2013 and 2014 were respectively 804 and 862 $m^3 \cdot s^{-1}$ at the N'Djamena station (i.e. runoff of 41 and 44 mm/y respectively). These two years are considered "wet" compared to the inter-annual average of 689 $m^3 \cdot s^{-1}$ (value calculated for the period 1985 to 2015, data source: DRE).

2.4. Reconstruction and validation of discharge data

Discharge data are essential to interpret hydro-geochemical behavior, to calculate weighted annual average concentrations, and to estimate chemical fluxes. A linear interpolation was used to fill the gaps in the Chari river discharge time series at the Chagoua station, in order to have a complete daily record for a hydrological year (2013-2014). These gaps occur mainly during low flow periods.

For the Logone, in the absence of gauging stations before the confluence of the two rivers, the flow data were reconstructed from a mass balance based on the Sr isotopic signature:

$$\left(\frac{^{87}Sr}{^{86}Sr}\right)_{CL} = \alpha \left(\frac{^{87}Sr}{^{86}Sr}\right)_{L} + (1-\alpha)\left(\frac{^{87}Sr}{^{86}Sr}\right)_{C}$$

where the subscripts CL, C and L point to the Chari-Logone, Chari and Logone respectively. α is the proportion of the Chari-Logone Sr isotopic signature coming from the Logone river, also corresponding to the Sr fluxes balance as follows:

$$\alpha = \frac{[\mathrm{Sr}]_{\mathrm{L}} * \mathrm{Q}_{\mathrm{L}}}{[\mathrm{Sr}]_{\mathrm{CL}} * \mathrm{Q}_{\mathrm{CL}}}$$

where Q is the river discharge. This method assumes that chemical fluxes are conservative. The Logone river discharge is then calculated as a function of α, Q_{CL}, and Sr concentrations measured in the Logone and in the Chari-Logone river water. This method is also used to calculate an independent Chari discharge value.

3. Results

3.1. Chemical and isotopic compositions

The conductivity measured on the field is well correlated with the alkalinity. However, the alkalinity obtained from the Chari in April 2013 appeared as an outlier, 20% above the value expected from the correlation and was ruled out, suspecting a a possible sample pollution after the water collection. The results of ionic and molecular concentrations and strontium isotopic composition of the Chari, Logone and Chari-Logone rivers are shown in Fig. 3 and in Tables 1, 2 and 3. Ionic proportions (Fig. 3) show that anion concentrations are largely dominated by HCO_3, which represents, whatever the station, more than 97% of the sum of the anions (in meq.L^{-1}), the remaining being represented by chloride (about 2.5% of the anion charge), while other anions NO_3 and SO_4 are often under the detection limit (Fig. 3). Cation concentrations (in

meq/L) are slightly dominated by Ca (34%), closely followed by Mg (29%), and Na (25%). K represents between 11 and 14% of the cationic composition. Dissolved silica represents an average of 0.152 ± 0.014 mmol/L.

Strontium data show higher concentrations and lower radiogenic signatures (0.0012 ± 0.0003 meq/L, n = 20; 0.7120 ± 0.0002, n = 20) for the Logone, compared to the Chari river (0.0009 ± 0.0003 meq/L, n = 20; 0.7170 ± 0.0005, n = 20) (Tables 1 to 3). The average for the Chari-Logone is 0.0010 ± 0.0003 meq/L (n = 20) and 0.7145 ± 0.0008 (n = 20).

3.2. Seasonal variations

Considering its dominance in anion concentration, HCO_3 can be considered as a good proxy of the global dissolved load. HCO_3 shows a minimum concentration during the rainfall season (July-August) (Fig. 4b). Then it increases until November-December and remains at high levels until the end of the dry season (March-April). Despite a higher average concentration compared to the other cations (Fig. 4c and 4d), Ca undergoes the strongest decrease during the rainfall season. This is particularly evident in the Chari river. In addition, the Ca/Na molar ratio shows a sharp drop during the beginning of the rainfall season, and then increases during the flood rise and the flood recession. In both rivers, the Ca/Na ratio also displays a small decrease synchronous with the maximum discharge (Fig.4e et a).

The strontium content shows the same pattern as other dissolved elements in the Chari and Logone rivers, and most particularly with a behavior similar to that of other alkaline earths elements (Ca and Mg): the highest values are observed in April and the lowest in July (Fig. 5a). The isotopic signature is rather stable over the period in the Logone and in the Chari. In contrast, the Chari-Logone isotopic signature is highly variable, as a result of the mixing between the two tributaries, with variable contributions along the year (Fig. 5b).

The Chari and Logone flow rates calculated using the Sr isotopic mass balance method are shown in Figure 5c. It led to values consistent with the Chari and the Chari-Logone measured river discharge.

4. Discussion

4.1. Contribution of silicate weathering to the dissolved load

4.1.1. Atmospheric contributions

The atmospheric contribution to the dissolved load is classically based on marine elemental ratios, assuming that chloride comes exclusively from atmospheric inputs. Thus, atmospheric contributions are estimated by:

$$X_{atm} = Cl_{riv} * \left(\frac{X}{Cl}\right)_{sea}$$

where X corresponds to any elemental concentrations, in seawater (*sea*), river water (*riv*) and atmospheric inputs (*atm*).

In the Chari and Logone rivers (Table 4), this calculation yields atmospheric Na concentrations between 12 and 14 µmol/L (i.e. 9.1 % of the total Na concentration), and low atmospheric input concentrations of other elements: 1 to 1.7 µmol/L for Mg (1.9%); 0.2 to 0.3 µmol/L for K (0.4%) and Ca (0.3%). These low atmospheric inputs show that the river geochemistry is dominated by continental weathering. The low atmospheric inputs together with the absence of saline rocks in the basin explain the very low Cl concentrations measured over the basin and in the Chari Logone (Bouchez et al. 2016).

4.1.2. A silicate weathering signature

In this section we attempt to elucidate the geological nature and the reservoirs responsible for the chemistry of the Chari-Logone basin.

Several studies implemented mixing methods based on the relationships between molar ratios (Ca/Na, Mg/Na, HCO_3/Na) to characterize the different poles (end-members) that can contribute to the dissolved charge of a river, namely the chemical weathering of the different lithological facies (carbonate rocks, silicate rocks and evaporitic rocks) (Négrel et al. 1993; Gaillardet et al. 1999; Picouet et al. 2002). This method relies on the idea that the water chemical composition carries a specific signature attributed to each altering rock, characterized by ionic ratios, which are conservative during evaporation and dilution processes. The river water composition results from the simple combination of these weathering signatures, depending on the lithological facies within a watershed (Négrel et al. 1993, Picouet et al. 2002), after removing the atmospheric contribution. The geochemical signatures of carbonate rocks,

silicate rocks or evaporitic rocks results from literature databases, and a global synthesis was proposed by Gaillardet et al. (1999).

Therefore, the proportion of the geological nature of the rocks presently weathered in the Chari-Logone catchment can be estimated using the annual average ratios of Ca/Na, Mg/Na and HCO3/Na of river water, compared to predefined end-members compositions based on the synthesis of Gaillardet et al. (1999). Mixing diagrams of ionic ratios corrected from atmospheric contributions were plotted and compared to worldwide river data (Fig. 6). The mean molar ratios of the Chari, the Logone and the Chari-Logone rivers are very low (e.g. for the Chari-Logone: Ca/Na = 0.85±0.19; Mg/Na = 0.63±0.10; HCO_3/Na = 4.2±0.58 and close to the composition of the silicate endmember taken from the synthesis of Gaillardet *et* al (1999): Ca/Na = 0.35 ± 0.15; Mg/Na = 0.24 ± 0.12; HCO_3/Na = 2 ± 1, despite a slight shift towards the carbonate endmember (Fig. 6). This could be due to the expected variability of the silicate end-member composition, as Gaillardet et al. (1999) underlined that the natural variations of silicate lithological facies could overcome the range defined by this end-member composition. In addition, although no carbonate formation outcrops in the southern part of the watershed, the presence of pedogenic carbonate nodules in the north of Cameroon has been observed, which formation relies on local sources of Ca coming from in situ weathering (Dietrich et al. 2017). These carbonate nodules are widespread in the Chari-Logone basin, and their dissolution, which could modify the molar ratio without modification of the Sr isotopic signature, may also explain this slight shift towards higher Ca/Na. Therefore, even if silicate weathering appears as the dominant process controlling the chemistry of the Chari-Logone River, in agreement with the geology, one could not rule out the contribution of secondary carbonate dissolution. This would imply a "local carbon cycle", in which atmospheric carbon consumption associated with the classical mechanism of silicate weathering, would be partly released during the weathering of secondary minerals.

4.1.3. Comparison with other African systems

Total dissolved solid (TDS: sum of SiO_2, Ca, Mg, Na, K, HCO_3, Cl and SO_4) represents 55 and 56 mg/L for the Chari and Logone respectively (Table 5). These values are very low, with the same magnitude as those of the Niger (Table 5), which watershed also corresponds to silicate geological formations. Table 6 shows the mean values in µmol/L and µeq/L of all dissolved chemical elements in relation to global and African river values. All these values of African rivers are below the world mean values obtained by Meybeck (2003).

The HCO_3 content of the Chari-Logone system is similar to that of the downstream Niger River, but higher than that of the Congo River and of the upper part of the Niger basin (Table 6). Dissolved silica is important to consider when estimating chemical denudation and CO_2 consumption, because its presence in solution is almost entirely due to silicate weathering (Négrel et al. 1993; Gaillardet et al. 1997; Amiotte Suchet et al. 2003; Harmon et al. 2016). It is predominant in the Chari and Logone rivers, with a mean annual value of 159 to 153 µmol/L respectively, which is similar to the average world river concentration of silica, but lower than for the Niger river. Except for the K concentration, the annual average levels of the other dissolved elements (Ca, Mg, Na) are lower than the overall mean value (Table 6). This low dissolved mineral value can be explained by the morphology of the flattened watershed and the nature of the already leached bedrock.

4.2. Concentration-discharge relationship at the seasonal scale

As described previously, there are strong seasonal variations in the concentrations of dissolved chemical elements in the Chari and Logone waters. The lowest concentrations are observed during the rainy season, suggesting a dilution effect by rainfall and rapid runoff, while the highest values are observed during the dry season, when the influence of evaporation is strong. When chemical concentrations are compared with river discharge, the relation shows a hysteresis loop, suggesting a non-linear behavior of the catchment (Fig. 7). This hysteresis behavior is well observed for Ca and Mg in the Chari and Logone rivers, and for Na in the Logone River while K shows constant concentrations throughout the year, except during the months of lowest discharge in April and May. Hysteresis behaviors between chemical elements and river flows are observed in several basins around the world (Walling and Foster 1975; Walling and Webb 1980; Probst et al. 1992; Evans and Davies 1998; Bravard and Petit 2000; Picouet et al. 2002; Calmels et al. 2011; Moquet et al. 2016; Bouchez et al. 2017; Ibarra et al. 2017). Some explanations involve the contribution of different reservoirs. For example, in the Niger Basin (Picouet et al. 2002) the hysteresis behavior was interpreted as: (1) a variable seasonal contribution of different flow sources (runoff, hypodermic flow, groundwater), (2) a delayed contribution of the various branches of the hydrographic network and (3) a flushing effect of the ponds with the new flood, which brings water that has been concentrated during the dry season. In addition, this flushing effect can also lead to the mobilization of soluble minerals deposited in the minor bed during the dry season, and on leaching of soil horizons.

For the Chari and Logone basins, the seasonal variations of the Ca/Na ratio indicate that different water sources are involved, in addition to the combined effects of dilution by rainfall and of concentration by evaporation. Nevertheless, the relationship between Ca/Na and discharge is more complex than a simple hysteresis loop: the discharge rising months p are characterized by an increase of Ca/Na, followed by a slight decrease at the flood maximum, and thereafter, the Ca/Na ratio remains constant during the flood recession, leading to a "double loop" (Fig. 7).

The highest constant Ca/Na ratios are observed during the low flow period (January-March), when river flow is supported by groundwater, while the lowest ratios are observed during the rainfall season, when rapid runoff dominates the water flow. Therefore, the variations of Ca/Na could result from the different residence time of water in the catchment.

As discussed above, the Ca/Na ratio reflects the geological nature of weathed formations. During the rainfall season, Ca/Na reaches a low value similar to that of the silicate end-member defined by Gaillardet et al. 1999 (Fig. 4-d). The increase of Ca/Na above this value may result from to the contribution of pedogenic carbonates weathering, thus more intense for longer residence time.

Then, the two-fold peak of Ca/Na could be attributed to the dual effect of 1) leaching and mobilisation of water that remained stored in the catchment, during the flood formation; and 2) groundwater signature, during the flood recession and low flow period. In between these two peaks, during the maximum discharge, the Ca/Na ratio displays intermediate values, resulting from the mixing between the two water sources.

The influence of groundwater signature during the flood recession in November-December, when the baseflow dominates river discharge, is also visible through stable elemental concentrations. From January until the beginning of the rainfall season, concentrations increase under the influence of evaporation. Then, when the rainfall season begins (April in the upper catchment), the persistent effect of evaporation compensates the dilution by rainfall. This explains that the Ca/Na ratio decreases together with the elemental concentrations, while the discharge remains low. The concentration of dissolved chemicals continue to decrease until July-August, consistently with the increase in discharge. This corresponds to the dilution of the river water by less concentrated water coming from precipitation. Discharge continues to increase until October while concentrations also increase. This can be attributed to the increasing contribution of more concentrated groundwaters, but also to the remobilization of chemical elements by the effect of land leaching by rains in the floodplains of Massenya for the Chari, and of Bongor and Yaeré for the Logone (Fig. 1).

This anti-clockwise hysteresis behavior well pronounced for Ca and Mg and less for Na and K is thus mainly driven by the contribution of two main water sources, rapid surface and subsurface water flow on one hand, and groundwater on other hand, i.e. “pre-event water”, which carry a higher Ca/Na signature.

4.3. Driving factors of silicate weathering fluxes

4.3.1. Annual average weathering fluxes in Chari and Logone sub-basins

The annual weighted average concentrations for 2013 were multiplied by the annual river discharge to calculate the annual total flux expressed in ton/y and specific flux ($g/m^2/y$) (Table 7). For the entire Chari-Logone basin, the TDS flux was estimated at 2.21 $g/m^2/y$. Despite its higher contribution, i.e. $1.38*10^6$ t/y, while the Logone provides $0.58*10^6$ t/y, the Chari river has a lower TDS specific flux, i.e. 1.59 $g/m^2/y$, compared to 6.16 $g/m^2/y$ for the Logone. Our data similar geochemical concentrations between the two rivers. Therefore, the observed difference in specific weathering flux is mainly due to runoff differences between the Chari (29 mm/y) and Logone (112 mm/y) river basins. This situation corresponds to transport-limited weathering regimes, also refered to as chemostatic behaviors, in which the runoff rate is the only factor controlling chemical fluxes (Godsey et al. 2009 and Koger et al. 2018).

4.3.2. Comparison with historical data on the Chari-Logone

To elucidate the question of the direct link between chemical and water fluxes, i.e. chemostatic behavior, it is interesting to compare our data with different magnitudes of runoff conditions, such as those that occurred during previous periods during the last 50 years. Dissolved loads and chemical fluxes were compared to data obtained in 1969, 1972 and 1973 (Gac 1980 and from Bouchez et al. 2016). The corresponding average annual flows (measured at station of N’Djamena on the Chari-Logone) were 1076 m^3s^{-1}, 577 m^3s^{-1} and 576 m^3s^{-1} in 1969, 1972 and 1973 respectively (Carmouze, 1976, Gac, 1980, Roche, 1980, Olivry et al., 1996). The year 1969 is the wettest of our data set and corresponds to the beginning of the so-called “Great Sahelian drought” of the 1970-1980 period. Fig. 8 presents a comparative study of dissolved loads between these pre-drought period and present day conditions. The sum of the cations (Ca + Mg + Na + K) varied in the range 8.7 to 14.4 mg/L in 1969 (Gac 1980; Roche 1980); 8.7 to 14.6 mg/L in 1972 (Carmouze 1976, Gac 1980) and 8.7 to 19.9 mg/L in 2013 (this study). The most variable concentrations are those encountered during the dry season (March-June), which

showed higher values in recent years, while the flood season (September-November) displayed surprisingly constant values, independently of the discharge magnitude (Fig. 8). The annual chemical flux is dominated by the flood season: even with higher concentrations during the low water period, the March-June period only contributes to 11% of the annual flux. Thus, the concentration variations observed during low flow periods have little effect on the annual flux. The comparison between historical and recent data shows that for the Chari-Logone system, the inter-annual variability of high flow concentrations is very low, even during the more humid years prior to the 1970s Sahelian drought. As the flood period dominates the total annual export, it can thus be concluded that the annual weathering load exported is directly related to the runoff.

4.3.3. Impact of semi-arid environments on the carbon cycle

In the strongly contrasted climatic context of the Chari basin, the very low average runoff (29 mm/y in 2013) is due to the fact that some sub-basins do not contribute to the runoff, especially in the Sahelian part of the catchment. Indeed, the chloride mass balance of the Chari-Logone basin showed that only 12 ± 8% of the catchment is connected to the main rivers (Bouchez et al. 2019). In many parts of the basin, evaporation encompasses all other fluxes, leading to endorheic situations where dissolved load is not exported to the outflow. These disconnected areas become productive during more humid periods, leading to a significant increase in chemical fluxes. In addition, the precipitation of secondary minerals, such as pedogenic carbonate nodules, may be enhanced in these endorheic areas.

Therefore, the impact of semi-arid areas on the carbon cycle are two-fold. First, there is a direct positive relationship between hydrological fluxes and atmospheric carbon consumption by silicate weathering. As the hydrological response to climate change is particularly amplified in semi-arid environments, the carbon flux response to climate may also be enhanced. Second, the hydrological closure, either local or at the catchment scale, implies that atmospheric carbon consumed by silicate weathering is stored inside the catchment, either in soils (e.g. pedogenic carbonates), either in lakes (e.g. secondary minerals produced by reverse weathering). Although evident, this assertion may have important global implication, since endorheic areas represent an important part of continental surfaces.

Conclusions

The Chari and Logone basins cover an area of approximately 613 000 km² and drain water from the northern flank of Adamaoua (Cameroon) and the Central African ridge, towards Lake Chad. The analysis of the distribution of the major elements showed that the Chari and Logone rivers are very poorly mineralized and that the dissolved load mainly comes from the weathering of silicates, although the Ca/Na ratio may reflect the influence of pedogenic carbonate dissolution. The isotope compositions of strontium confirm the absence of a significant primary carbonate pole on the basin. Substantial seasonal variations of river concentrations are observed, with higher concentrations during the dry season and lower concentrations during the rainy season, but with a delay of about 2 months between the rainfall peak and the flood peak. In the Chari-Logone basin, we observed that concentrations follow an annual hysteresis, related to a variable contribution over time of surface water and groundwater.

Based on the $^{87}Sr/^{86}Sr$ ratios, we estimated that the Chari and the Logone rivers respectively contributed to 59 % and 41% of the total dissolved load to Lake Chad. Silicate weathering largely dominated the dissolved load. A flux of $5.9 * 10^5$ tons/y of dissolved materials transported to Lake Chad was estimated downstream of N'Djamena for the year 2013. The Chari Logone Basin follows a chemostatic behavior. Therefore, the inter-annual variations of dissolved loads reaching Lake Chad are directly related to the variations in the Chari-Logone discharge.

Acknowledgments

This work was supported by the French National Research Institute for Sustainable Development (IRD) in the framework of the project 'Préservation du Lac Tchad: Contribution à la stratégie de développement du lac' funded by 'Fond Français de l'Environnement Mondial' and by 'Agence Française pour le Développement'. The authors are grateful to the University of N'Djamena, the Centre National de la Recherche pour le Développement of Chad (CNRD) and the French Embassy in Chad for their logistical support. We thank Hélène Mariot for the preparation of the chemistry and the analysis of the major elements and Abel Guihou for the analysis of the isotopic composition of strontium.

References

Agbri L, Bamba S, Doumouya I, Savane I (2010) Bilan des flux de matières particulaires et dissoutes du Sassandra à Gaoulou pont (Côte d'Ivoire). Sci Nat 7:107–118. doi:10.4314/scinat.v7i2.59944

Amiotte Suchet P, Probst J-L, Ludwig W (2003) Worldwide distribution of continental rock lithology: Implications for the atmospheric/soil CO2 uptake by continental weathering and alkalinity river transport to the oceans. Glob Biogeochem Cycles 17. doi:10.1029/2002GB001891

Béné, C., Neiland, A., Jolley, T., Ovie, S., Sule, O., Ladu, B., Mindjimba, K., et al. (2003) Inland fisheries, poverty, and rural livelihoods in the Lake Chad Basin. J. Asian Afr. Stud. 38(1), 17–51. doi:https://doi.org/10.1177/002190960303800102

Bouchez C, Goncalves J, Deschamps P, et al (2016) Hydrological, chemical, and isotopic budgets of Lake Chad: a quantitative assessment of evaporation, transpiration and infiltration fluxes. Hydrol Earth Syst Sci 20:1599–1619. doi: 10.5194/hess-20-1599-2016.

Bouchez J, Moquet J-S, Espinoza JC, et al (2017) River mixing in the Amazon as a driver of concentration-discharge relationships. Water Resour Res 53:8660–8685. doi:10.1002/2017WR020591

Bouchez C, Deschamps P, Goncalves J, et al (2019) Water transit time and active recharge in the Sahel inferred by bomb-produced 36 Cl. Scientific Reports 9:7465. doi:10.1038/s41598-019-43514-x

Bravard J-P, Petit F (2000) Les cours d'eau: dynamique du système fluvial. https://www.persee.fr/doc/ingeo_0020-0093_1998_num_62_2_2583_t1_0093_0000_1

Cabot J (1965) Le bassin du moyen Logone. Document de ORSTOM, P.355, Paris. https://www.persee.fr/doc/ingeo_0020-0093_1965_num_29_5_5777

Calmels D, Galy A, Hovius N, et al (2011) Contribution of deep groundwater to the weathering budget in a rapidly eroding mountain belt, Taiwan. Earth Planet Sci Lett 303:48–58. doi: 10.1016/j.epsl.2010.12.032

Carmouze J-P (1976) La régulation hydrogéochimique du lac Tchad: Contribution à l'analyse biogéodynamique d'un système lacustre endoréique en milieu continental cristallin. doc. ORSTOM, Paris, p.413. http://horizon.documentation.ird.fr/exl-doc/pleins_textes/pleins_textes_6/Tra_d_cm/08443.pdf

Chorover J, Derry LA, McDowell WH (2017) Concentration-Discharge Relations in the Critical Zone: Implications for Resolving Critical Zone Structure, Function, and Evolution. Water Resour Res 53:8654–8659. doi.org/10.1002/2017WR021111

Dietrich F, Diaz N, Deschamps P, et al (2017) Origin of calcium in pedogenic carbonate nodules from silicate watersheds in the Far North Region of Cameroon: Respective contribution of in situ weathering source and dust input. Chem Geol 460:54–69. doi.org/10.1016/j.chemgeo.2017.04.015

Drever JI, Zobrist J (1992) Chemical weathering of silicate rocks as a function of elevation in the southern Swiss Alps. Geochim Cosmochim Acta 56:3209–3216. doi: 10.1016/0016-7037(92)90298-W

Evans C, Davies TD (1998) Causes of concentration/discharge hysteresis and its potential as a tool for analysis of episode hydrochemistry. Water Resour Res 34:129–137. doi: 10.1029/97WR01881

Gac J-Y (1980) Géochimie du bassin du lac Tchad: Bilan de l'altération de l'érosion et de la sédimentation, doc. ORSTOM, Paris, p.252. http://www.documentation.ird.fr/hor/fdi:00039

Gaillardet J, Dupre B, Allegre CJ, Négrel P (1997) Chemical and physical denudation in the Amazon River Basin. Chem Geol 142:141–173. https://doi.org/10.1016/S0009-2541(97)00074-0

Gaillardet J, Dupré B, Louvat P, Allegre CJ (1999) Global silicate weathering and CO2 consumption rates deduced from the chemistry of large rivers. Chem Geol 159:3–30. doi.org/10.1016/S0009-2541(99)00031-5

Godsey SE, Kirchner JW, Clow DW (2009) Concentration–discharge relationships reflect chemostatic characteristics of US catchments. Hydrological Processes: An International Journal 23:1844–1864. DOI: 10.1002/hyp.7315

Harmon RS, Wörner G, Goldsmith ST, et al (2016) Linking silicate weathering to riverine geochemistry—A case study from a mountainous tropical setting in west-central Panama. Bulletin 128:1780–1812. doi:10.1130/B31388.1

Hartmann J, Jansen N, Dürr HH, et al (2009) Global CO2-consumption by chemical weathering: What is the contribution of highly active weathering regions? Glob Planet Change 69:185–194. doi:10.1016/j.gloplacha.2009.07.007

Ibarra DE, Moon S, Caves JK, et al (2017) Concentration–discharge patterns of weathering products from global rivers. Acta Geochim 36:405–409. doi: 10.1007/s11631-017-0177-z

Koger JM, Newman BD, Goering TJ (2018) Chemostatic behaviour of major ions and contaminants in a semiarid spring and stream system near Los Alamos, NM, USA. Hydrol Process 32:1709–1716. DOI: 0.1002/hyp.11624

Louis P (1970) Contribution géophysique à la connaissance géologique du bassin du lac Tchad. ORSTOM, Paris. http://www.documentation.ird.fr/hor/fdi:04616

Louvat P, Allègre CJ (1997) Present denudation rates on the island of Reunion determined by river geochemistry: basalt weathering and mass budget between chemical and mechanical erosions. Geochim Cosmochim Acta 61:3645–3669. doi.org/10.1016/S0016-7037(97)00180-4

Meybeck M (2003) Global occurrence of major elements in rivers. Treatise Geochem 5:207–223. doi:10.1016/B0-08-043751-6/05164-1

Meybeck, M. (1987) Global chemical weathering of surficial rocks estimated from river dissolved loads. Am. J. Sci. 287(5), 401–428. doi:10.2475/ajs.287.5.401

Milliman JD, Meade RH (1983) World-wide delivery of river sediment to the oceans. J Geol 91:1–21. doi:10.1086/628741

Moquet J-S, Crave A, Viers J, et al (2011) Chemical weathering and atmospheric/soil CO2 uptake in the Andean and Foreland Amazon basins. Chem Geol 287:1–26. https://doi.org/10.1016/j.chemgeo.2011.01.005

Moquet J-S, Guyot J-L, Crave A, et al (2016) Amazon River dissolved load: temporal dynamics and annual budget from the Andes to the ocean. Environ Sci Pollut Res 23:11405–11429 . DOI: 10.1007/s11356-015-5503-6

Musolff A, Schmidt C, Selle B, Fleckenstein JH (2015) Catchment controls on solute export. Adv Water Resour 86:133–146. DOI: 10.1016/j.advwatres.2015.09.026

Négrel P, Allègre CJ, Dupré B, Lewin E (1993) Erosion sources determined by inversion of major and trace element ratios and strontium isotopic ratios in river water: The Congo Basin case. Earth Planet Sci Lett 120:59–76. doi: 10.1016/0012-821X(93)90023-3

Olivry J-C, Diallo Iam M, Bricquet J-P (1994) Quelques données préliminaires sur l'environnement et la qualité des apports du Niger au Sahel. https://www.researchgate.net/publication/32972541_Premiers_resultats_sur_la_mesur

e_des_flux_de_matieres_dissoutes_et_particulaires_dans_les_apports_du_Niger_au_Sahel

Ollivier P, Hamelin B, Radakovitch O (2010) Seasonal variations of physical and chemical erosion: A three-year survey of the Rhone River (France). Geochim Cosmochim Acta 74:907–927. DOI: 10.1016/j.gca.2009.10.037

Pias J (1968) Contribution à l'étude des formations sédimentaires tertiaires et quaternaires de la cuvette tchadienne et des sols qui en dérivent (République du Tchad). PhD Thesis, Orstom. Retrieved from http://horizon.documentation.ird.fr/exldoc/pleins_textes/cahiers/PTP/18537.PDF

Picouet C, Dupré B, Orange D, Valladon M (2002) Major and trace element geochemistry in the upper Niger river (Mali): physical and chemical weathering rates and CO2 consumption. Chem Geol 185:93–124. DOI: 10.1016/S0009-2541(01)00398-9

Probst J-L, NKounkou R-R, Krempp G, et al (1992) Dissolved major elements exported by the Congo and the Ubangi rivers during the period 1987–1989. J Hydrol 135:237–257. doi.org/10.1016/0022-1694(92)90090-I

Roche M-A (1980) Traçage naturel salin et isotopique des eaux du système hydrologique du lac Tchad. ORSTOM, Paris, p.391/ Retrieved fromhttp://www.documentation.ird.fr/hor/fdi:00328

Schneider J-L, Wolf JP (1992) Carte géologique et hydrogéologique de 1/500 000 de la republique du Tchad, mémoire explicatif. BRGM, p.531, Paris

Schuster, M., Roquin, C., Duringer, P., Brunet, M., Caugy, M., Fontugne, M., Mackaye, H. T., et al. (2005) Holocene lake Mega-Chad palaeoshorelines from space. *Quat. Sci. Rev.* **24**(16–17), 1821–1827. DOI: 10.1016/j.quascirev.2005.02.001

Sylvestre F., (2014) Variabilité paléohydrologique et changements climatiques, *In* Lemoalle J., Magrin G. (dir.) : *Le développement du lac Tchad : situation actuelle et futurs possibles*, Marseille, IRD Editions, coll. Expertise collégiale : 79-92.

Thirlwall MF (1991) Long-term reproducibility of multicollector Sr and Nd isotope ratio analysis. Chem Geol Isot Geosci Sect 94:85–104. doi:10.1016/0168-9622(91)90002-E

Tipper ET, Bickle MJ, Galy A, et al (2006) The short term climatic sensitivity of carbonate and silicate weathering fluxes: insight from seasonal variations in river chemistry. Geochim Cosmochim Acta 70:2737–2754. doi.org/10.1016/j.gca.2006.03.005

Viers J, Dupré B, Braun J-J, et al (2000) Major and trace element abundances, and strontium isotopes in the Nyong basin rivers (Cameroon): constraints on chemical weathering processes and elements transport mechanisms in humid tropical environments. Chem Geol 169:211–241. doi.org/10.1016/S0009-2541(00)00298-9

Walling DE, Foster IDL (1975) Variations in the natural chemical concentration of river water during flood flows, and the lag effect: some further comments. J Hydrol 26:237–244. https://doi.org/10.1016/0022-1694(75)90005-0

Walling DE, Webb BW (1980) The spatial dimension in the interpretation of stream solute behaviour. J Hydrol 47:129–149. doi.org/10.1016/0022-1694(80)90052-9

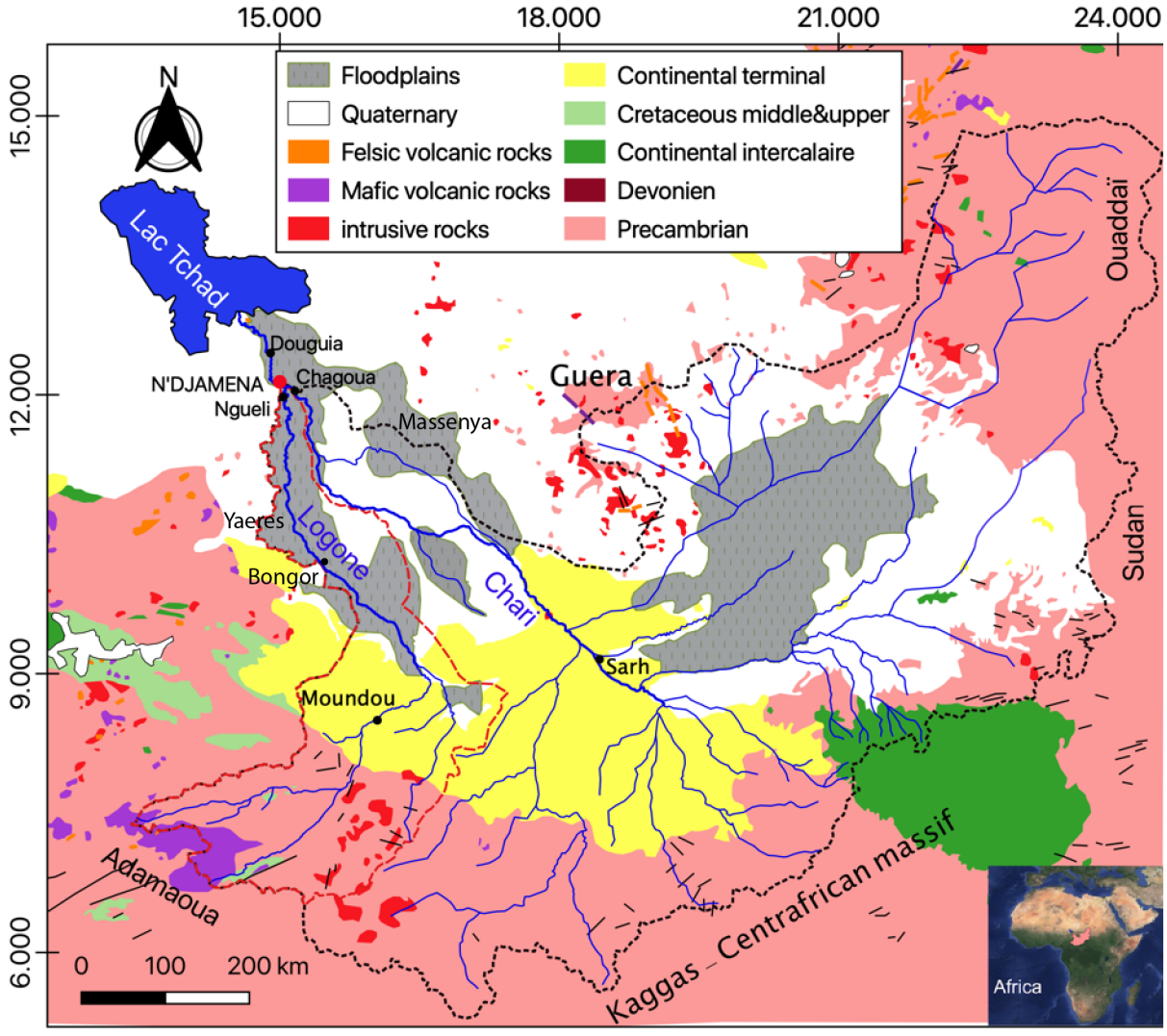

Figure 1. Geological map of the Chari-Logone basin (Louis 1970), with sample locations (Ngueli, Chagoua and Douguia). The black dotted line represents the boundary of the Chari-Logone basin and the red dotted line the boundary of the Logone basin.

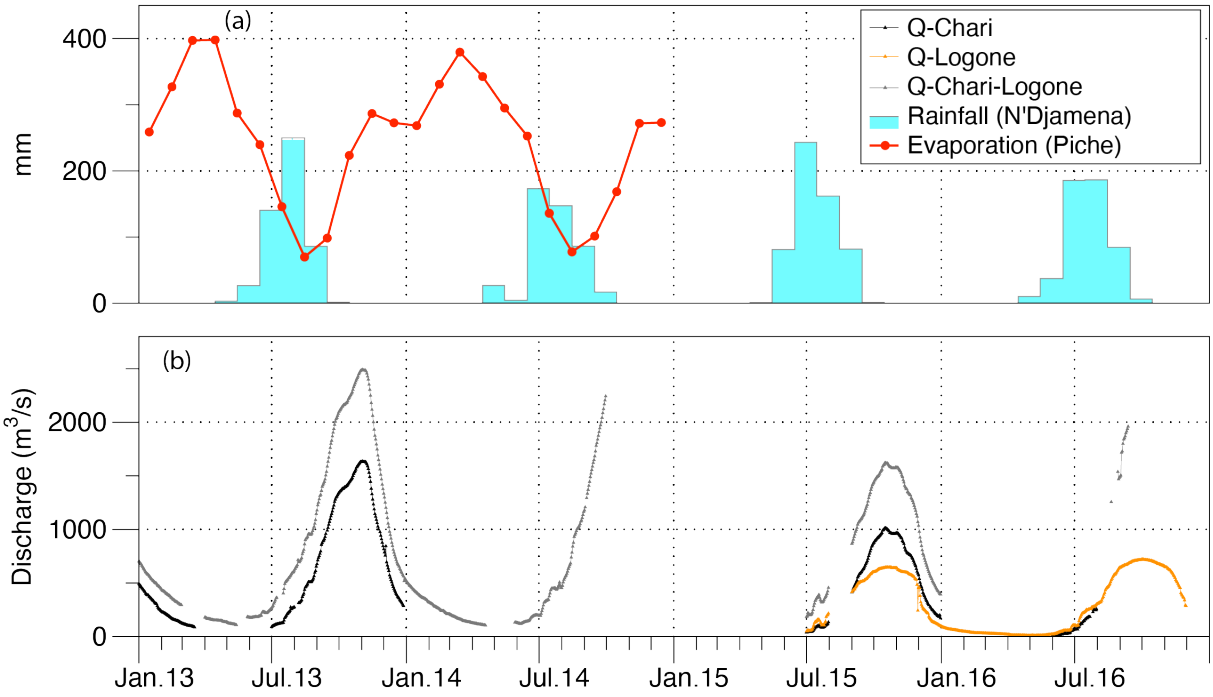

Figure 2: Monthly rainfall and evaporation (Piche method) at the N'Djamena station (a); daily discharge (b): the black dotted curve represents the flow of the Chari river at Chagoua before the confluence, the yellow curve represents the flow of Logone river at Ngueli and the grey curve is the flow of Chari - Logone river after the confluence of the two rivers Chari and Logone measured at N'Djamena.

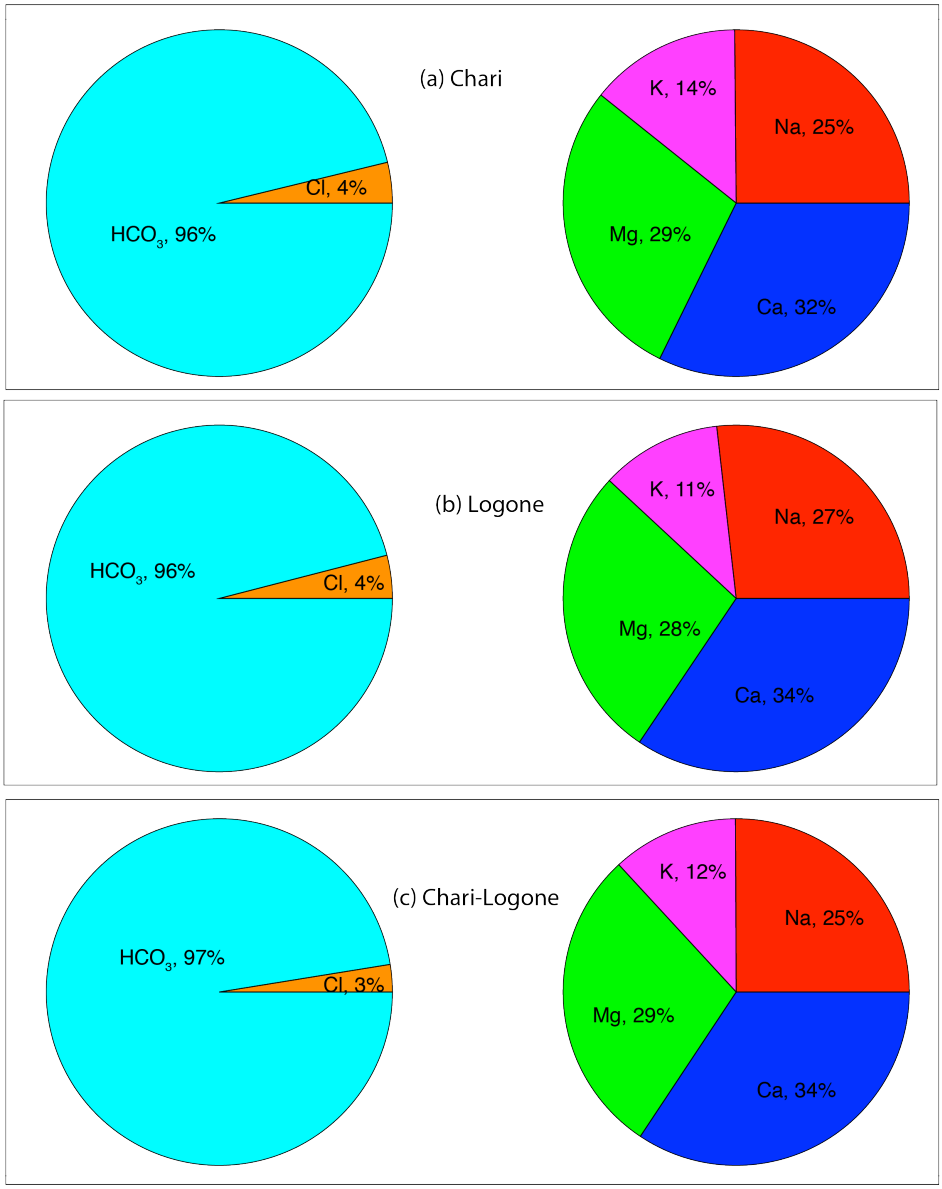

Figure 3. Ionic compositions (average annual proportion of each anion and cation in meq/L) of the Logone, Chari and Chari-Logone waters.

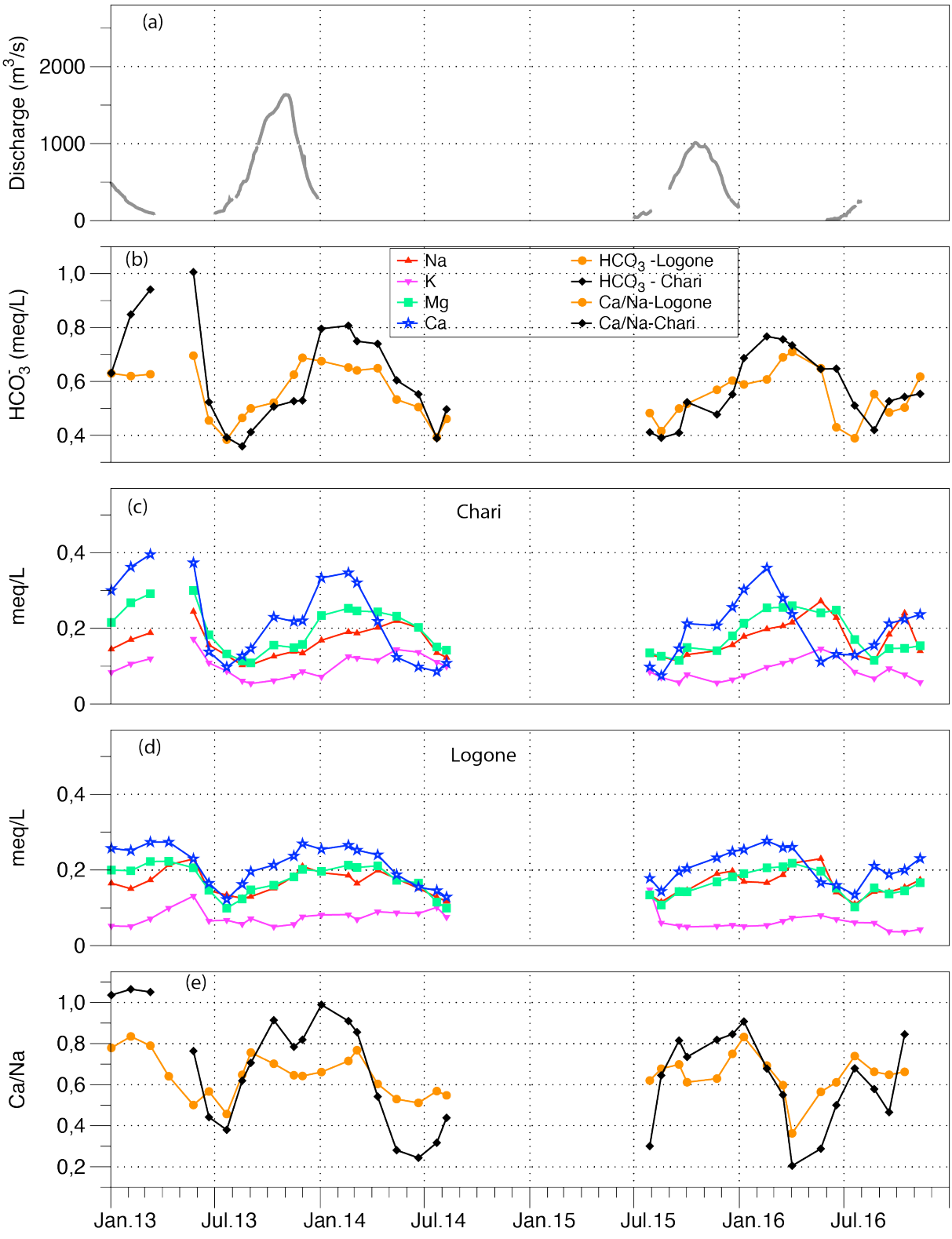

Figure 4 : Seasonnal evolution of ionic concentrations and Ca/Na molar ratio in the Chari and Logone rivers between 2013 and 2016. The Chari-Logone discharge provides the seasonal flood framework.

627

628

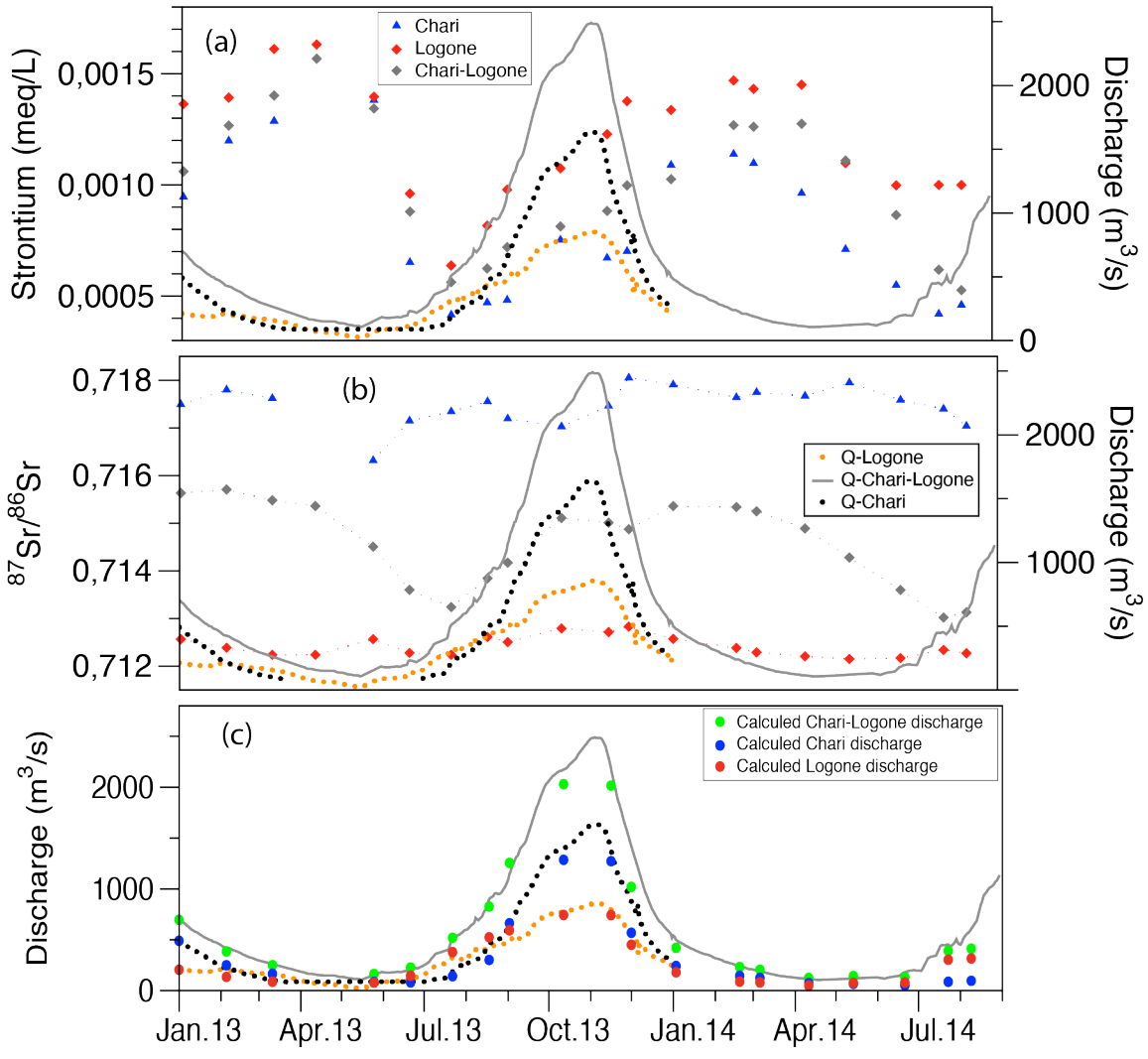

629

630 Figure 5: Concentration (a) and isotopic composition (b) of strontium in the Chari (blue),
631 Logone (red) and Chari – Logone (grey) water. As in Fig. 2, the grey curve and the black dotted
632 curve are the measured Chari-Logone and Chari river discharges, respectively. The grey dotted
633 curve is the Logone discharge deduced from the difference between the Chari - Logone and
634 Chari data. The colored circles are the flows rates calculated from the strontium isotope ratios
635 mass balance for the Logone (red), Chari (blue), and sum of both values (green).

636

637

638

639

640

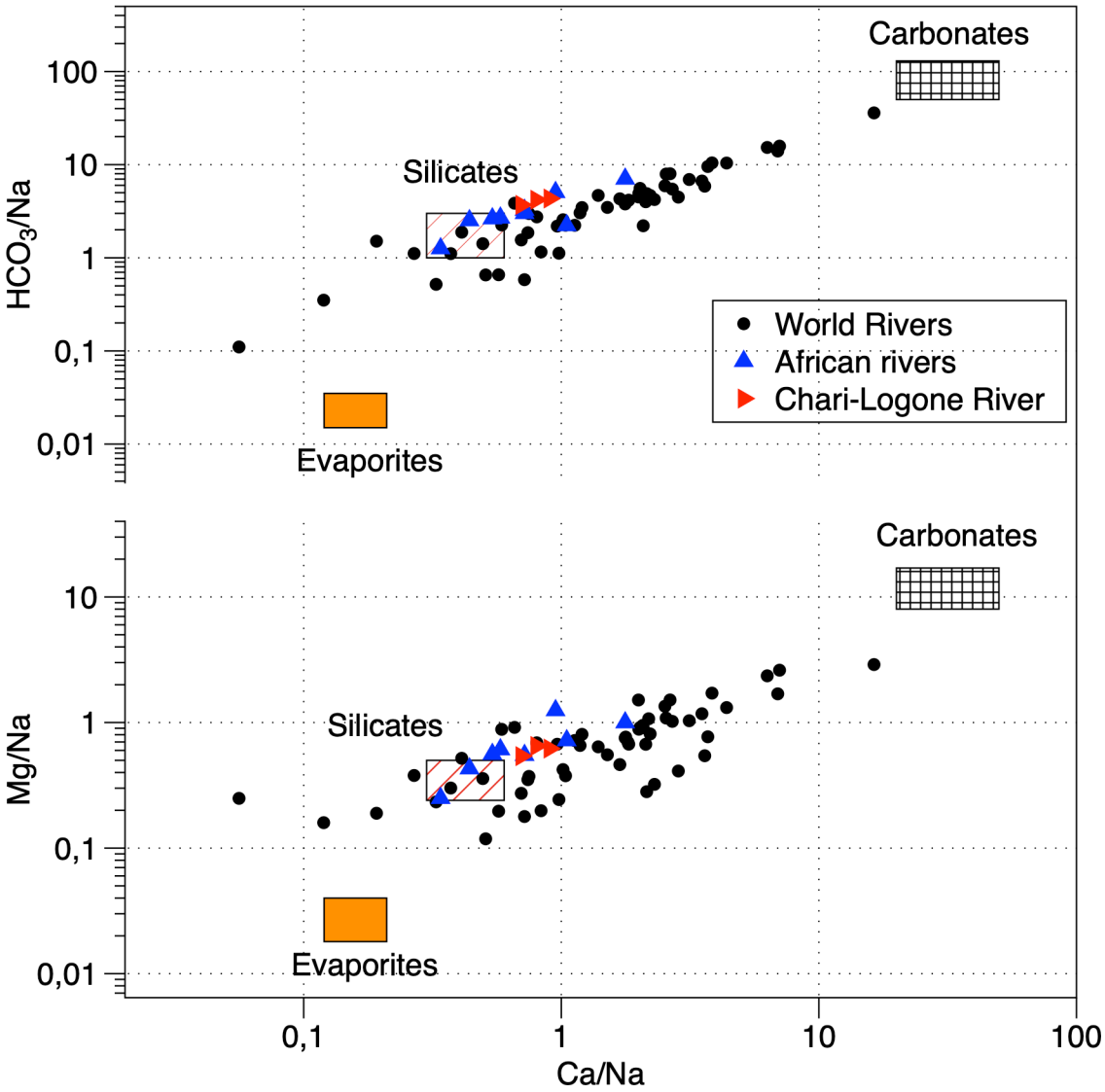

Figure 6: Mixing diagram showing concentration ratios in river water, and in weathering end-members defined in previous studies. The values of the Ca/Na, Mg/Na and HCO_3/Na ratios of the silicate, carbonate, and evaporitic end-members are taken from Gaillardet et al. (1999). The data of the various world and African rivers plotted in this diagram are taken from Gaillardet et al. (1997) , Meybeck (2003), Picouet et al. (2002), Orange (1996) and Agbri et al. (2010).

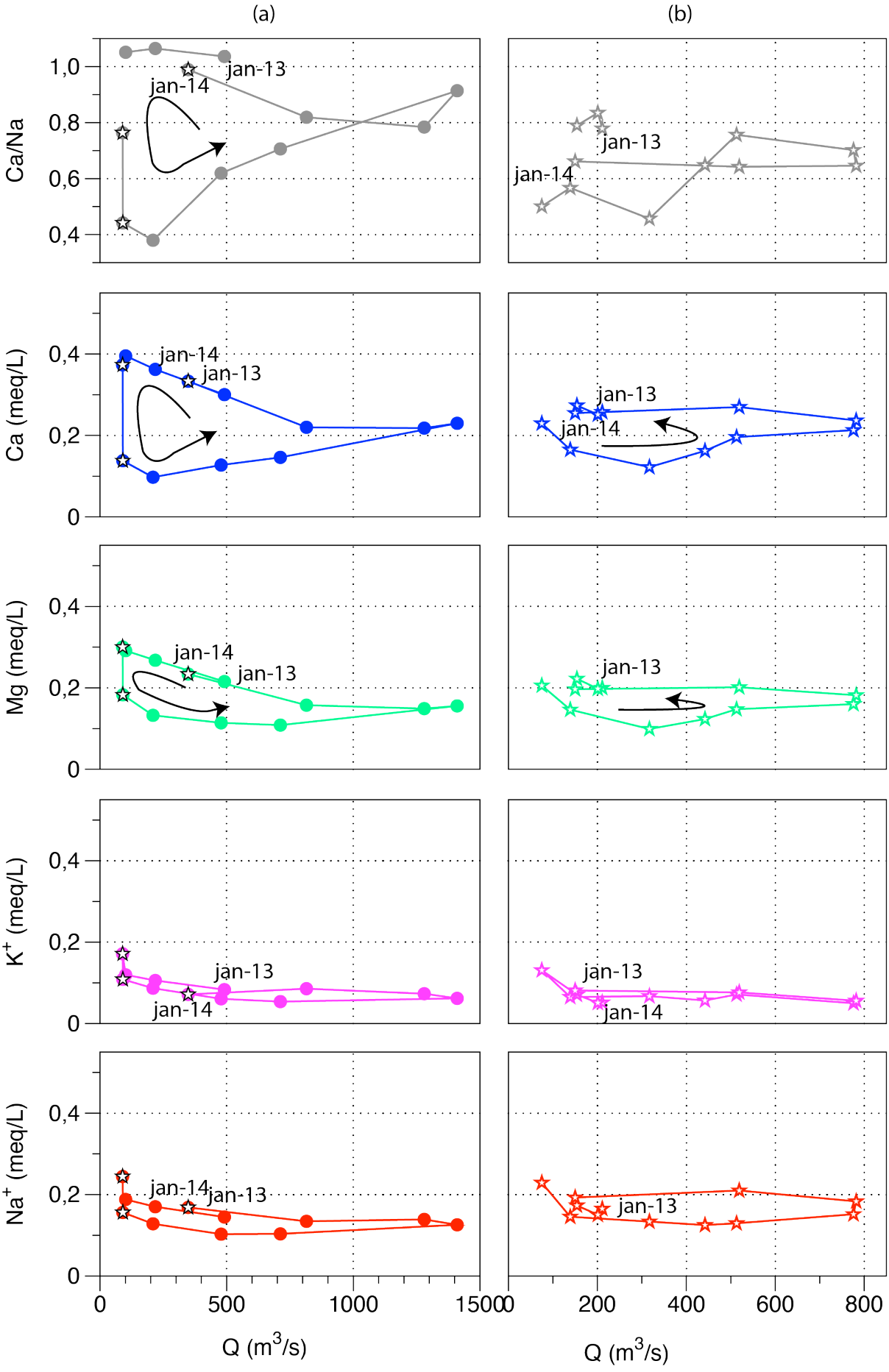

653

Figure 7: Evolution of ionic concentrations (Ca, Mg, K and Na) as a function of the discharge flow of the Chari (a) and the Logone (b) rivers over the 2013-2014 period. Stars correspond to reconstituted flows.

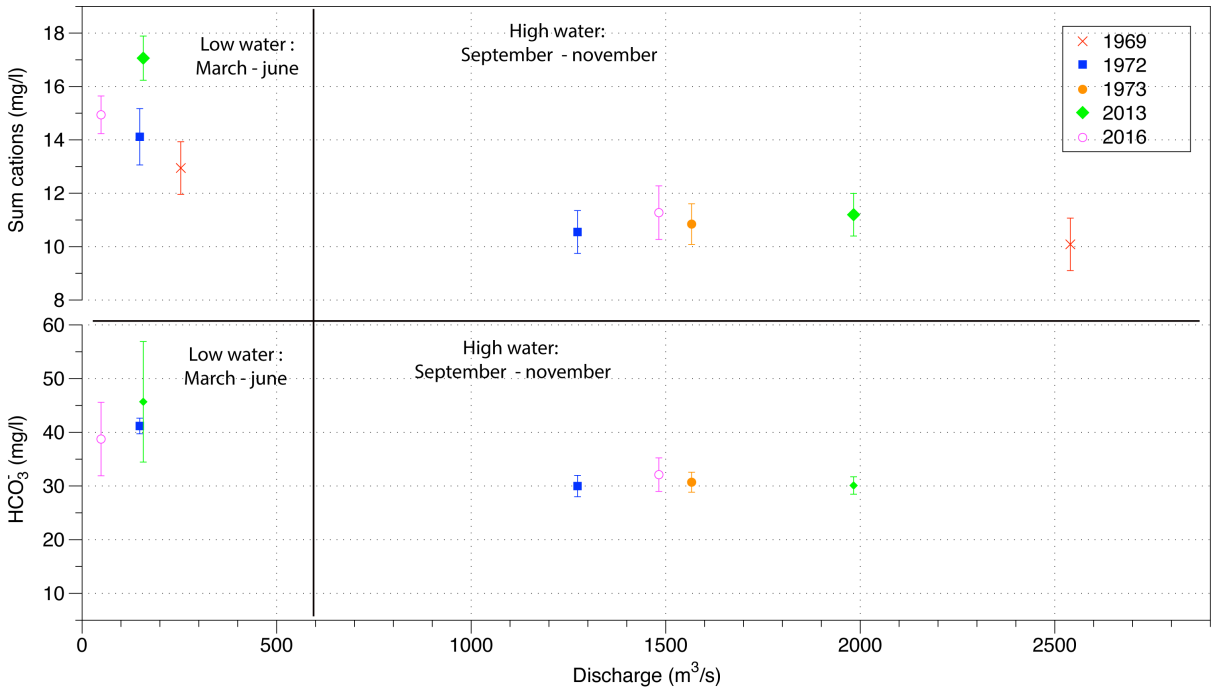

Figure 8: Average concentrations of the Chari-Logone river corresponding to the two main periods of an annual cycle: low water period (March-June) and high water (flood) period (September-November), compared to 1969, 1972 and 1973 data (from Gac 1980).

Table 1: Measured concentrations in Chari River monthly water samples

Dates	Q -mesured	Q -calculated	EC	pH	T	$^{87}Sr/^{86}Sr$	SiO_2	Na^+	K^+	Mg^{2+}	Ca^{2+}	Sr^{2+}	Cl^-	SO_4^{2-}	HCO_3^-	Ionic B.
	(m^3/s)	(m^3/s)	µs/cm		°C					mmol/L (SiO_2) and µeq/L (other elements)						
02/01/2013	365	490	74	8,3	22,0	0,7175	155	145	83	215	300	0,9	11	2	631	8,2
05/02/2013	177	250	89	7,9	24,0	0,7178	136	170	106	268	362	1,2	17	1	849	3,3
11/03/2013	104	165	98	8,3	26,8	0,7176	142	188	120	291	395	1,3	26	2	941	2,8
12/04/2013	79		108	8,4	29,0											
25/05/2013	54	85	98	9,1	32,0	0,7163	161	244	172	300	373	1,4	65	12	1006	4,0
21/06/2013	113	81	57	10,8	29,1	0,7172	103	156	109	183	138	0,7	22	8	523	5,6
22/07/2013	164	142	43	8,5	30,6	0,7173	70	128	87	133	97	0,4	18	6	392	6,3
18/08/2013	459	302	38	8,1	29,7	0,7176	161	103	61	114	127	0,5	10	7	359	6,0
02/09/2013	1022	663	41	8,1	29,3	0,7172	163	104	54	109	146	0,5	8	7	412	0,0
12/10/2013	1472	1286	57	7,6	29,3	0,7170	143	126	62	156	230	0,8	11	2	506	6,2
16/11/2013	1312	1273	55	8,1	25,1	0,7175	150	139	73	149	218	0,7	19	0	527	4,7
01/12/2013	499	569	62	8,2	26,9	0,7181	147	134	86	157	220	0,7	14	5	529	6,1
03/01/2014	384	242	81	7,7	23,9	0,7179	140	168	72	234	333	1,1	13	0	796	0,7
19/02/2014	159	145	85	8,5	23,7	0,7176	165	191	125	253	347	1,1	43	3	807	6,3
06/03/2014	71	125	84	8,9	24,7	0,7178	161	187	121	246	321	1,1	41	1	749	7,8
11/04/2014	51	74	78	7,4		0,7177	160	202	116	243	219	1,0	29	5	740	2,6
14/05/2014	47	68	69	9,0	28,7	0,7180	102	220	144	232	124	0,7	30	3	604	8,7
21/06/2014	64	52	59	8,9	29,2	0,7176	159	201	137	202	98	0,5	51	6	553	7,2
23/07/2014	59	87	47	8,8	29,2	0,7174	146	135	110	151	86	0,4	12	13	389	10,8
09/08/2014	681	97	44	8,8	28,0	0,7170	71	123	99	142	108	0,5	38	16	497	-2,5
29/07/2015			88	7,3	27,2			129	85	135	98	0,5	21	8	411	0,7
18/08/2015			57	7,3	30,7			124	70	126	75	0,4	16	5	391	-2,0
18/09/2015			51	7,6	31,8			114	57	115	146	0,5	7	6	410	1,1
02/10/2015			63	8,0	31,0			130	78	149	213	0,7	9	3	523	3,1
23/11/2015			74	7,5	24,3			141	56	141	207	0,7	8	0	478	5,7
20/12/2015			77	7,8	21,2			156	64	180	256	0,8	10	3	552	7,5
09/01/2016			89	8,1	22,8			179	75	213	302	0,9	11	5	687	4,4
18/02/2016			97	8,4	25,0			198	98	254	360	1,1	13	2	767	7,5
17/03/2016			85	8,7	27,1			206	108	255	280	1,1	22	3	756	4,0
02/04/2016			84	8,8	24,4			216	116	260	237	1,1	27	4	734	4,0
22/05/2016			77	9,0	34,8			272	146	241	111	0,6	30	6	646	5,8
18/06/2016			75	9,0	32,6			228	131	248	131	0,8	33	8	647	3,5
20/07/2016			74	8,3	31,0			129	85	170	129	0,8	20	8	511	-2,3
23/08/2016			56	7,6	32,8			114	67	116	155	0,6	9	7	420	1,8
18/09/2016			65	7,2	31,0			184	94	146	213	0,7	35	6	527	5,7
15/10/2016			76	7,2	31,9			240	77	147	224	0,7	67	3	543	5,8
11/11/2016			62	9,2	27,8			140	57	154	237	0,8	8	4	554	1,9

676 Table 2: Measured concentrations in Logone River monthly water samples

Dates	Q -calculated	EC	pH	T	$^{87}Sr/^{86}Sr$	SiO_2	Na^+	K^+	Mg^{2+}	Ca^{2+}	Sr^{2+}	Cl^-	SO_4^{2-}	HCO_3^-	Ionic B.
	(m^3/s)	µs/cm		°C	mmol/L (SiO_2) and μeq/L (other elements)										
02/01/2013	206	66	8,5	21,3	0,7126	151	165	52	200	257	1,4	10	2	630	3,4
05/02/2013	135	64	8,2	22,7	0,7124	164	150	51	198	251	1,4	14	4	620	2,4
11/03/2013	87	69	7,9	26,0	0,7122	179	173	71	222	274	1,6	19	1	627	8,3
12/04/2013		72	8,4	29,0	0,7122	185	214	99	223	274	1,6	52	3		
25/05/2013	78	72	8,4	31,7	0,7126	178	229	131	206	230	1,4	66	4	696	6,7
21/06/2013	147	55	8,5	29,1	0,7123	130	146	65	146	165	1,0	21	11	455	6,9
22/07/2013	379	37	8,2	30,1	0,7122	139	134	67	99	122	0,6	26	8	384	4,8
18/08/2013	525	48	8,4	29,2	0,7126	146	125	57	123	162	0,8	10	8	465	0,3
02/09/2013	593	53	8,1	29,0	0,7125	142	130	72	148	196	1,0	18	3	500	4,3
12/10/2013	744	55	7,5	29,8	0,7128	133	152	50	160	213	1,1	13	1	521	4,9
16/11/2013	743	63	8,7	26,8	0,7127	157	183	56	182	237	1,2	14	1	625	2,6
01/12/2013	451	72	7,5	27,3	0,7128	159	210	77	202	270	1,4	23	7	688	4,9
03/01/2014	180	83	8,3	22,9	0,7126	170	193	81	197	255	1,3	35	0	675	3,6
19/02/2014	88	66	7,4	23,1	0,7124	180	186	82	213	265	1,5	44	0	652	6,8
06/03/2014	81	68	8,4	24,0	0,7123	175	164	69	207	252	1,4	27	3	641	3,9
11/04/2014	51	77	8,7	29,1	0,7122	184	199	90	211	240	1,5	36	5	649	6,5
14/05/2014	76	59	8,8	29,4	0,7122	160	177	87	172	188	1,1	49	9	533	7,9
21/06/2014	80	55	8,5	30,7	0,7122	167	152	85	166	155	1,0	38	6	505	5,0
23/07/2014	304	46	8,2	31,5	0,7123	146	128	101	115	146	0,8	43	12	393	11,0
09/08/2014	316	41	9,1	28,2	0,7123	132	117	75	99	129	0,6	28	10	461	-4,6
29/07/2015		65	7,3	28,3			134	148	134	178	1,0	81	15	483	0,1
18/08/2015		92	7,4	30,2			116	60	107	143	0,8	12	3	416	-0,5
18/09/2015		66	7,1	30,4			144	52	143	195	1,0	7	2	499	2,5
02/10/2015		59	10,4	33,0			146	50	143	204	0,9	7	4	517	1,3
23/11/2015		80	7,3	24,7			190	52	169	233	1,0	10	2	569	5,0
20/12/2015		80	8,6	21,1			197	54	182	249	1,0	14	8	603	4,3
09/01/2016		74	8,2	22,5			169	51	190	254	1,2	12	6	589	4,6
18/02/2016							166	54	206	277	1,2	15	2	607	5,9
17/03/2016		74	8,4	27,8			187	65	208	259	1,3	19	4	690	0,5
02/04/2016		76	8,3	25,1			218	74	218	261	1,3	21	6	709	2,3
22/05/2016		68	8,8	31,2			230	80	197	167	1,1	25	7	649	-0,5
18/06/2016		54	8,4	29,3			141	70	152	160	0,9	18	9	430	6,7
20/07/2016		56	8,2	29,9			110	61	102	134	0,7	12	10	389	-0,6
23/08/2016		61	7,3	31,4			142	60	153	211	1,0	8	1	553	0,3
18/09/2016		64	7,8	32,0			142	37	137	188	1,0	6	0	485	1,4
15/10/2016		65	7,1	31,5			154	36	145	200	0,9	6	0	503	2,5
11/11/2016		76	7,9	27,1			174	43	166	231	1,1	6	2	618	-1,0

677

678 Table 3: Measured concentrations in Chari-Logone River monthly water samples

Dates	Q -mesured (m^3/s)	Q -calculated (m^3/s)	EC µs/cm	pH	T °C	$^{87}Sr/^{86}Sr$	SiO_2	Na^+	K^+	Mg^{2+}	Ca^{2+}	Sr^{2+}	Cl^-	SO_4^{2-}	HCO_3^-	Ionic Balance %
										mmol/L (SiO_2) and µeq/L (other elements)						
01/01/2013	702	696	70	8,2	20,7	0,7156	158	145	72	207	282	1,1	9	2	650	4,2
11/02/2013	385	385	84	8,0	22,5	0,7157	160	167	93	250	336	1,3	16	4	791	3,3
12/03/2013	251	251	87	8,1	24,3	0,7155	153	182	99	269	347	1,4	21	2	851	2,7
07/04/2013	165		92	8,0	28,5	0,7154	163	192	111	296	356	1,6	24	3	891	3,4
26/05/2013	169	164	80	8,1	30,3	0,7145	172	220	107	256	242	1,3	26	3	770	3,5
23/06/2013	221	228	54	8,3	28,4	0,7136	164	149	83	169	156	0,9	21	8	483	7,2
23/07/2013	534	520	39	8,0	29,1	0,7132	128	111	62	105	116	0,6	15	4	378	2,1
17/08/2013	915	827	43	8,2	28,2	0,7138	147	117	60	114	138	0,6	12	0	399	3,7
03/09/2013	1251	1256	46	8,2	28,6	0,7142	147	115	69	128	170	0,7	20	5	468	1,4
10/10/2013	2174	2030	53	7,5	29,9	0,7151	145	116	53	150	211	0,8	3	3	492	3,8
17/11/2013	2001	2016	56	7,6	26,3	0,7150	156	145	52	161	221	0,9	4	0	520	5,2
08/12/2013	1022	1020	62	7,0	26,9	0,7149	171	154	57	181	241	1,0	6	2	579	4,5
04/01/2014	491	421	66	8,3	21,0	0,7154	163	148	64	197	259	1,0	10	0	642	2,0
22/02/2014	232	233	79	8,4	21,7	0,7153	169	167	83	238	308	1,3	16	0	736	3,9
03/03/2014	200	205	79	7,8	23,3	0,7153	170	167	83	235	297	1,3	17	0	748	2,2
12/04/2014	114	125	75	8,2	27,5	0,7149	170	189	93	241	235	1,3	21	3	655	7,3
11/05/2014	119	144	68	8,4	29,0	0,7143	118	192	93	226	174	1,1	4	1	614	5,4
08/06/2014	126	133	56	7,6	30,0	0,7136	164	162	90	187	123	0,9	23	7	491	6,7
20/07/2014	448	391	39	8,1	28,2	0,7130	140	112	63	107	114	0,6	42	5	327	9,5
02/08/2014	475	413	44	8,1	28,3	0,7131	98	95	55	96	104	0,5	12	11	385	-4,9
30/07/2015			50	7,2	28,0			125	77	124	150	0,7	21	15	470	-3,1
19/08/2015			66	7,1	29,5			118	62	103	130	0,6	13	7	412	-2,3
19/09/2015			60	7,2	30,7			132	56	130	173	0,8	11	4	458	1,9
03/10/2015			63	7,6	31,0			137	64	145	204	0,8	8	2	516	2,3
22/11/2015			73	7,5	24,1			167	53	152	215	0,8	9	3	526	4,3
21/12/2015			73	7,9	19,0			170	60	180	249	0,9	11	6	582	4,8
10/01/2016			76	8,3	20,5			174	66	204	287	1,1	12	8	637	5,4
19/02/2016			82	8,4	23,8			188	79	232	311	1,2	15	3	708	5,4
18/03/2016			79	8,8	27,2			197	86	231	261	1,1	20	4	716	2,2
04/04/2016			81	8,5	25,4			219	93	239	234	1,2	24	2	731	1,8
22/05/2016			69	8,5	29,9			251	103	202	127	0,7	30	5	602	3,4
22/06/2016			57	8,5	29,4			161	82	167	145	0,9	24	10	491	2,8
22/07/2016			60	8,4	29,2			114	65	107	131	0,7	14	13	417	-3,0
24/08/2016			57	7,9	30,2			122	64	127	172	0,7	6	6	480	-0,8
19/09/2016			58	6,6	31,2			125	49	133	195	0,7	7	0	474	2,3
16/10/2016			71	7,6	33,6			134	49	138	204	0,7	4	0	529	-0,9
12/11/2016			70	8,3	26,3			149	50	155	231	0,8	5	1	576	0,2

679

680

Table 4: Contribution of rainfall inputs in the Chari-Logone water.

	Na	K	Ca	Mg
	%			
Logone	9.2	0.5	0.3	2.1
Chari	9.0	0.3	0.2	1.8

Table 5: Synthesis of dissolved flux of water, and total dissolved solids (TDS) in the upper Niger basin (Picouet et al 2002) and in the Chari-Logone basin.

Rivers	Runoff (mm/y)	TDS (mg/L)	TDS ($g/m^2/y$)
Douna (Niger)	70	45.6	3.2
Banankoro (Niger)	331	41.9	13.9
Chari	29	55.4	1.6
Logone	112	55.5	6.2
Chari-Logone	41	54	2.2

Table 6: Ionic elemental concentration (µeq/L) and (µmol/L) for silica of the Chari-Logone basin, the Upper Niger (Picouet *et al.,* 2002), the Congo basin and the world weighted average (Meybeck & Ragu, 1987; Meybeck, 2003).

Rivers	Area	Discharge	Runoff	SiO_2	Na	K	Mg	Ca	Cl	SO_4	HCO_3	Σ^+	Σ^-	Data source
	km^2	km^3/y	mm/y	µmol/L	µeq/L	µeq/L	µeq/L	µeq/L	µeq/L	µeq/L	µeq/L	µeq/L	µeq/L	
World weighted average of rivers				145	240	44	245	594	167	175	798	1123	1140	Meybeck 2003
Niger (Niamey)	1 200 000	154	128	233	78	28	156	276	26	5	549	538	580	Meybeck et Ragu 1987
Logone (Ngueli)	90 000	10	112	148	159	62	164	213	17		539	598	556	This work
Chari (Chagoua)	523 000	15	29	148	133	73	156	215	14		524	577	538	This work
Chari-Logone (Douguia)	613000	25	41	152	133	62	159	210	10		523	564	533	This work
Upper Niger (Koulikoro)	120 000	33	273	203	124	45	86	114	23		360	370	383	Picouet et al. 2002
Congo (Zaïre)	3 700 000	1200	324	157	96	43	118	112	37	15	258	369	310	Meybeck et Ragu 1987

Table 7: Total dissolved solid (TDS) specific fluxes (SiO_2 + Na + K + Ca + Mg + HCO_3) and specific weathering rates (SiO_2 + Na + K + Ca + Mg) in African rivers. Logone, Chari and Chari–Logone data are obtained from this study and data for other rivers are from Meybeck and Ragu (1987), Picouet *et* al. (2002) and Meybeck (2003).

Rivers	Area	Discharge	Runoff	SiO_2	Na	K	Mg	Ca	Cl	SO_4	HCO_3	Total disolveed specifique flux	Specific altération	Data source
	(km^2)	(km^3/y)	mm/y	$g/m^2/y$	$g/m^2/y$	$g/m^2/y$	$g/m^2/y$	$g/m^2/y$	$g/m^2/y$	$g/m^2/y$	$g/m^2/y$	$g/m^2/y$	$g/m^2/y$	
World weighted average of rivers	-	-	-	2.98	1.88	0.6	1.01	4.04	2	2.87	16.54	31.92	15.38	Meybeck 2003
Upper Niger (Koulikoro)	120 000	32.76	273	3.48	0.78	0.48	0.56	1.33	0.23	-	5.99	12.87	6.88	Picouet et al. 2002
Congo (Zaire)	3 700 000	1200	324.32	3.05	0.72	0.54	0.46	0.78	0.43	0.48	5.10	11.56	6.45	Meybeck et Ragu 1987
Niger (Niamey)	1 200 000	154.1	128.42	1.80	0.23	0.14	0.24	0.76	0.12	0.06	4.30	7.65	3.35	Meybeck et Ragu 1987
Logone (Nguéli)	90 000	10.04	111.56	1,00	0.41	0.27	0.22	0.51	0.07	0.02	3.66	6.16	2.50	This work
Chari-Logone (Douguia)	613000	25.34	41.34	0.38	0.13	0.1	0.08	0.19	0.01	-	1.32	2.21	0.89	This work
Chari (Chagoua)	523 000	15.3	29.25	0.26	0.09	0.083	0.06	0.14	0.01	0.01	0.93	1.59	0.66	This work